Jonathan R. Lamontagne
Advisor: Jery R. Stedinger
HRF Final Research Report
10/20/13

Executive Summary

This report summarizes research that I conducted with Hydro Research Foundation (HRF) support. The general focus was hydropower operations optimization using dynamic programming (DP) algorithms. More specifically, there were three areas of concern. The first concern was near real-time operations optimization using a time decomposition algorithm with different representations of uncertainty. The second concern was the value of forecasts and forecast precision to operations optimization. The third concern is the reduction of the computational burden of high-dimensional DP using intelligent sampling of the state space. Idealized reservoir systems based on the Kennebec River in Maine are used as case studies.

The objective of hydropower operations optimization is to maximize the expected benefit obtained from a reservoir system from the present time to the end of some planning horizon. In practice time is often broken into decision stages, so the problem becomes the selection of a sequence of releases which maximizes the expected benefit, subject to a set of constraints. The problem is challenging because the future availability of water is uncertain and the benefits and constraints are non-linear in the decision variable. Stochastic DP (SDP) algorithms are well suited to this type of problem. This research used the sampling SDP algorithm, which represents uncertain future flows as a range of flow time series scenarios rather than a Markov process.

The first concern addressed in this report is use of a time decomposition algorithm to optimize operation of a reservoir with a sub-daily time step. This involves solving nested optimization models, each with a different planning horizon and time-step, where the longer-term planning models inform the shorter-term models. This allows for rapid optimization of short-term operations, while efficiently considering seasonal objectives and constraints. A key consideration is how uncertainty is represented in each of the nested optimization models. By changing the probability of transitioning from one scenario to another, it is possible to generate a number of decision trees and the assessment of which is most advantageous. Three general transition cases were tested: the case which considers no transitions between scenarios, the case that assumes transitioning to any scenario is equally likely, and the case that bases the probability of transitioning on the flow forecast for the next period.

Through testing on an idealized single reservoir system, it was discovered that use of forecasts to estimate transition probabilities is most useful in short-term optimization. In fact, long- and mid-term

forecasts provide little improvement over configurations which allow no transitions between scenarios. In contrast, models that assume transition to any scenario is equally likely performed poorly, because they poorly reflect the persistence of flow when computing the long-term future value of water. Thus, it seems a successful algorithm configuration will use forecasts for short-term planning and a reasonable model of the persistence of flow for the long- and medium-term models (i.e. no transitions between scenarios or transitions based on forecasts).

The second research concern is the value improved forecast precision to optimization performance, and how this might change depending on the planning horizon and time step considered. For example, does the precision of long-term forecasts significantly affect the performance of the time decomposition algorithm, or is the precision of short-term forecasts more important. This is examined by applying the same model configurations previously described, but with varying forecast precision. It was determined that for summer operations optimization, long- and mid-term forecast precision contributes very little to the efficient operation of the reservoir. As was discussed above, use of forecasts for long- and mid-term planning is of little value, thus it is not surprising that forecast precision for longer-term planning is not important. In contrast, the performance of the algorithm is highly sensitive to the precision of the short-term forecast.

The third research concern is the reduction of the computational burden of high-dimensional DP. In DP, the state of the system in any time is described by state variables. In reservoir optimization, the state variable is reservoir storage, so the addition of a reservoir to the system involves the addition of a state variable, and a new dimension to the state space. This exponentially increases the difficulty of numerically solving the optimization problem. However, many points in the state-space represent unreasonable combinations of storages. The proposed Corridor DP algorithm saves computational effort by focusing the optimization effort on the region of the state space which the system will likely visit. One challenge of implementing Corridor DP is that cubic spline interpolation can perform poorly when basis points are irregularly placed. Instead, this research used radial basis function (RBF) interpolation, which is not constrained by the placement of basis points. Because the Corridor DP optimizes over the entire state space, not just inside the corridor, a coarse spline is fit to a few points in the extremes of the state space. An RBF surface models the deviation from the spline in the corridor region.

The Corridor DP algorithm is applied to an idealized four reservoir system. The corridor region was determined through simulation of the historic operation of the actual system. In numerical trials, an early implementation of the Corridor DP algorithm achieves a given relative error with about 1/2 the computational effort of DP with spline interpolation, and only 1/10 the computational effort of DP with

linear interpolation. Theoretical results are presented which suggest how the radial basis function interpolation and corridor selection criteria might be improved in the future.

This report focuses on the research conducted with HRF support. This research has focused on three concerns. First, the merit of various representations of uncertainty. Second, the value of forecast precision to the optimization effort. Finally, the reduction of the computational burden of solving high-dimensional DP problems. Results addressing each concern are presented, as well as suggestions for future work,

Before ending this executive summary, I'd like to express my gratitude to the Hydro Research Foundation for their support over the last three years. In addition to the financial support, they have provided many industry and government contacts who have proved invaluable as this research has evolved.

Section 1: Introduction

The objective of hydropower operations optimization is to maximize the expected benefit obtained from a reservoir system from the present time to the end of some planning horizon. In practice time is often broken into decision stages, so the problem becomes the selection of a sequence of releases which maximizes the expected benefit, Z. The incremental benefit in decision stage t, B_t, is a function of the reservoir storage, S_t, the reservoir release, R_t, and the inflow into the reservoir, Q_t. Let T be the index of the final decision stage in the planning horizon, and ν be the terminal value function. The terminal value function gives the value of storage in the reservoir after the planning horizon (after decision stage T), and is a function of S_{T+1}. The expected benefit from reservoir operations is

$$Z = E\left[\sum_{t=1}^{T} B_t(S_t, R_t, Q_t) + \nu(S_{T+1})\right] \quad (1)$$

The expectation in the definition of Z is necessary because hydrologic inflows are stochastic. In competitive energy markets, such as the New England ISO, the price of energy is also uncertain, a fact which will be ignored for the present discussion.

The hydropower operations optimization problem is focused on maximizing Z, subject to a set of constraints. Constraints can include the physical limitations of the powerhouse, environmental or regulatory limitations on the range of allowable releases, or some limitation associated with the electrical system. The benefit might be financial (see Faber and Stedinger, 2001) or some measure of reservoir efficiency (see Becker and Yeh, 1974). In the case that k multiple reservoirs are to be simultaneously

optimized as a system, R_t, S_t, and Q_t become $k \times 1$ vectors, and the problem generally becomes more complex.

Many mathematical techniques have been proposed to maximize Z. For a general review of optimization techniques commonly applied in reservoir optimization see Labadie (2004). This work is focused on stochastic dynamic programming (SDP) and sampling SDP (SSDP), which are well suited to the reservoir optimization problem and have been widely applied (Labadie, 2004). SDP and SSDP are described in more detail in Section 3. This research seeks to build on the body of SDP and SSDP work by addressing three research concerns.

The first concern addressed in this report is use of a time decomposition algorithm to optimize operation of a reservoir with a sub-daily time step. This involves solving nested optimization models, each with a different planning horizon and time-step, where the longer-term planning models inform the shorter-term models. This allows for rapid optimization of short-term operations, while efficiently considering seasonal objectives and constraints. A key consideration is how uncertainty is represented in each of the nested optimization models. By changing the probability of transitioning from one scenario to another, it is possible to generate a number of decision trees and the assessment of which is most advantageous. Three general transition cases were tested: the case which considers no transitions between scenarios, the case that assumes transitioning to any scenario is equally likely, and the case that bases the probability of transitioning on the flow forecast for the next period. Numerical testing is used to determine the relative merits of a range of model configurations. These results are described in Section 4.

The second research concern is the value of forecast precision in the context of the time decomposition algorithm. Flow forecasts can be used to estimate the likelihood that a future scenario will occur. This raises the question: how much does forecast precision affect optimization performance? A second question is whether the importance of forecast precision changes depending on the time step and planning horizon considered. For example, does the precision of long-term forecasts significantly affect the performance of the time decomposition algorithm, or is the precision of short-term forecasts more important. This is examined by applying the same model configurations previously described, but with varying forecast precision. This work is described in more detail in Section 5.

The third research concern is the reduction of the computational burden of high-dimensional DP. In DP, the state of the system in any time is described by state variables. In reservoir optimization, the state variable is reservoir storage, so the addition of a reservoir to the system involves the addition of a state variable, and a new dimension to the state space. This exponentially increases the difficulty of numerically solving the optimization problem. However, many points in the state-space represent

unreasonable combinations of storages. The proposed Corridor DP algorithm saves computational effort by focusing the optimization effort on the region of the state space which the system will likely visit. One challenge of implementing Corridor DP is that cubic spline interpolation can perform poorly when basis points are irregularly placed. Instead, this research used radial basis function (RBF) interpolation, which is not constrained by the placement of basis points. Because the Corridor DP optimizes over the entire state space, not just inside the corridor, a coarse spline is fit to a few points in the extremes of the state space. An RBF surface models the deviation from the spline in the corridor region. The Corridor DP algorithm is developed in more detail in Section 6.

The Kennebec River hydropower system is used as a case study for each of the three research concerns. Section 2 describes the hydrology of the Kennebec River Basin and the characteristics of the installed hydropower infrastructure along the river and its tributaries. Section 2 also describes the procedures used to generate synthetic inflow data for the reservoirs, and the two hypothetical systems which were used as case studies. It was necessary to generate synthetic data because the Kennebec system is privately owned and hydrologic data is proprietary.

Finally, Section 6 of this report contains some concluding remarks, as well as some indication of the future direction the research is expected to take.

Section 2: The Kennebec River

This section describes two hypothetical hydropower systems which are based on the Kennebec River in Maine. The original plan was to obtain flow and reservoir characteristic data from the system operator, NextEra Energy. Unfortunately, it proved impossible to obtain data directly from NextEra. However, there are a number of USGS gauges in the basin and adjacent basins, and most important plant characteristics can be obtained from Federal Energy Regulatory Commission (FERC) re-licensing documentation or other public sources. Section 2.1 describes the Kennebec River and the associated hydroelectric system, and Section 2.2 describes the hypothetical systems which were used in the preliminary research, and the procedures used to generate synthetic inflows.

Section 2.1: The Kennebec River

The Kennebec River basin is located in north-central Maine in the eastern United States. The river originates near the US/Canada border and flows 150 miles to the Atlantic Ocean at Merrymeeting Bay. The river has a drainage area of 5,870 square miles and includes a wide range of topography from mountains in the headwaters to flat coastal plains. The major tributaries are the Moose, Dead, Carrabassett, Sandy, and Sebasticook Rivers. The average gradient of the main channel is 8.5 feet per

mile, while the Dead and Sandy Rivers have channel gradients of 25 and 22 feet per mile respectively. The average annual discharge of the Kennebec River is 287.5 billion cubic feet (bcf) [Kennebec Water Power Co. (KWPC)].

The average annual temperature in the basin is 42° F, with average monthly temperatures ranging from nearly 70° F in July to 10° F in January. Extremes in the basin have ranged from 90° F to -30° F, with rapid changes in daily weather a common occurrence. The land cover is 8% agriculture, 75% wooded, 5% lakes and ponds, with the remaining 12% consisting of other land use, such as residential, urban, and industrial [KWPC]. The majority of the 'other' land use is in the lower reaches of the basin, as the headwaters are largely undeveloped.

The Kennebec River basin generally receives a large winter snowpack [Hodgkins et al., 2005], and the spring snowmelt represents the most significant feature of the annual hydrograph. For example, nearly 60% of the annual inflow to Flagstaff Lake on the Dead River occurs between March and May. To accommodate the spring freshet, the large storage reservoirs in the headwaters of the Kennebec are typically drawn down to 30% of full rated capacity [KWPC]. The arrival of the spring thaw varies from year to year, and is often marked by the 'ice out' date. Historically, the 'ice out' date is early May for the storage reservoirs in the headwaters, although a recent study suggests global warming is causing earlier 'ice out' [Hodgkins et al., 2002].

A major hydrologic consideration during the summer months is strong and localized thunderstorms. It is not uncommon for spatial variability to cause one basin to receive twice as much rainfall from a storm as an adjacent basin [KWPC]. This can cause difficulty when managing a network of storage reservoirs: where the rain falls might be more important than how much falls. On average, the basin receives between 40-50 inches of rain a year, with higher elevations often receiving more [National Atlas, 2005].

The role of evaporation and transpiration on the annual water balance are relatively minor. During an average summer, evaporation losses for the largest reservoirs are generally on the order of 1-1.5 feet of lake level. Combined with transpiration, summer time losses are as high as 81% of precipitation, however losses during the fall and winter months (when most of the precipitation falls), are much lower, so on an annual water balance they account for very small losses. In fact, evapo-transporation losses are often neglected in optimization efforts in this region [Cote, 2011].

Section 2.2.1: The Kennebec Hydropower System

There are ten hydro-electric generation facilities as well as two storage-only reservoirs (Moosehead and Flagstaff Lakes) located along the length of the river. The elevation change from the first facility to the last is 1073 vertical feet. The total installed hydro-electric generation capacity is 256 MW. The available storage in the Kennebec's three primary reservoirs, Moosehead Lake, Flagstaff Lake, and Brassua Lake is 44.7 billion cubic feet, or about 15% of the average annual runoff. Figure 1 shows a schematic of the Kennebec Hydropower system.

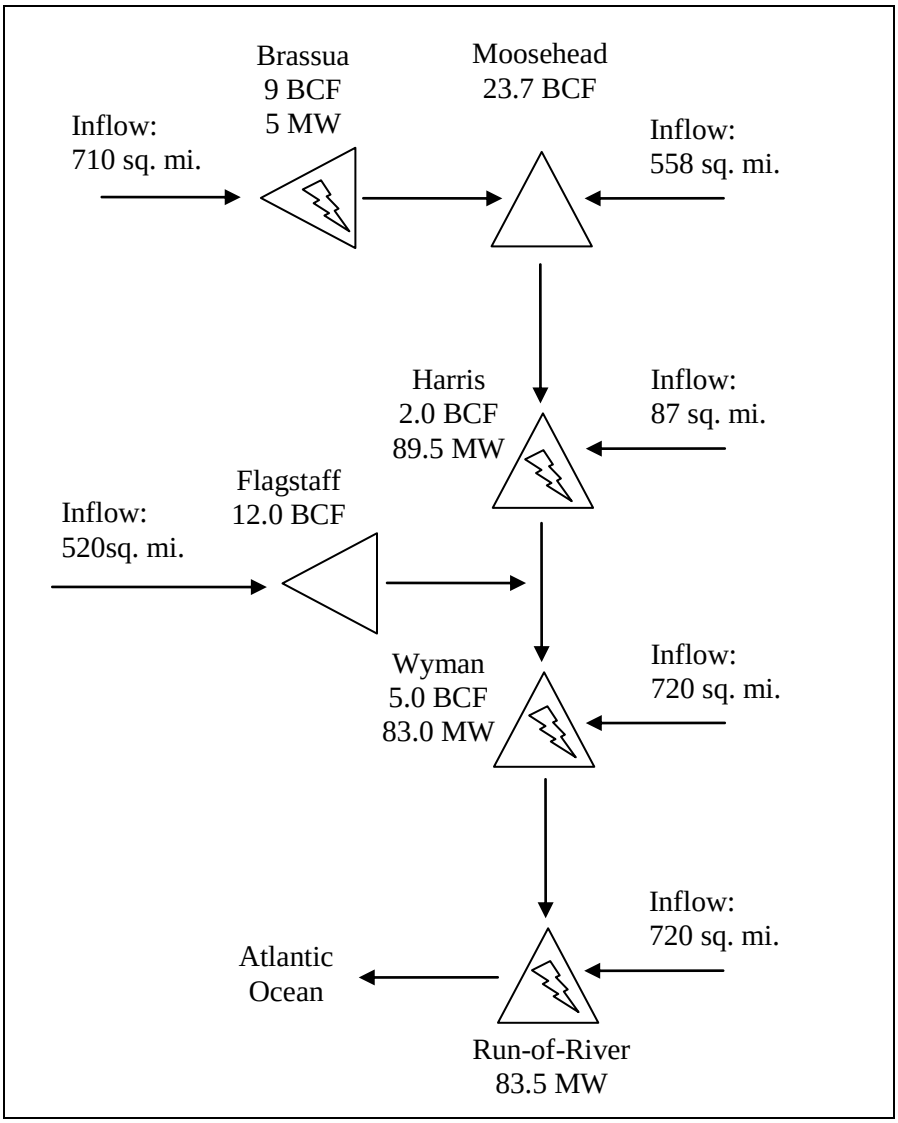

Figure 1: Schematic of the Kennebec Hydropower System

Essentially the system contains three storage reservoirs and two generating reservoirs, followed by seven run-of-river plants. Run-of-river plants have virtually no storage so the only water available in stage t is the inflow.

Section 2.2.2: Hypothetical Systems and Synthetic Hydrology

The majority of the Kennebec system is owned and/or operated by NextEra Energy. At the outset of this research it seemed that hydrologic and plant data would be available for the major projects on the Kennebec. Unfortunately, much of this data is proprietary, and it proved impossible to arrive at an arrangement to obtain the necessary data. Since this research is largely an academic exercise, we deemed it appropriate to study hypothetical basins resembling subsets of the real Kennebec System. As long as the characteristics and hydrology of the hypothetical systems approximately match the actual system, this should provide reasonable study basins for the proposed methodologies.

Two hypothetical system configurations were created: System A and System B. System A has a single reservoir and is created by imagining Harris Station with no upstream regulation (see Figure 2). System B has four reservoirs, consisting of Brassua, Flagstaff, an aggregation of Moosehead and Harris, and Wyman Station (see Figure 3). System B is used in the Corridor DP work described in Section 5.

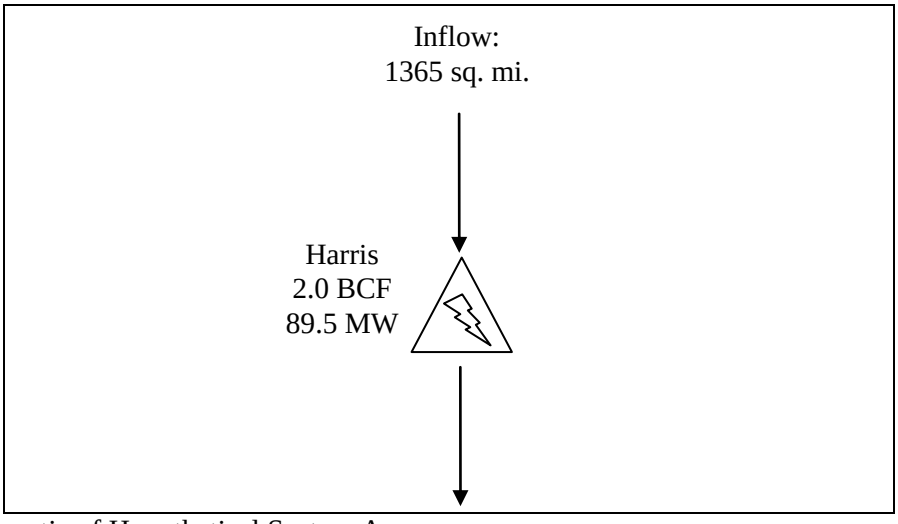

Figure 2: Schematic of Hypothetical System A

Plant and reservoir storage relationships for most of the system's facilities are available in the FERC relicensing materials. Additionally, information on the installed units were available through Oak Ridge National Lab. These data were sufficient to build fairly accurate representations of plant characteristics.

Obtaining reservoir inflow data was more complicated. Regulation on the main-stem of the Kennebec River started as early as the 1830's, so obtaining natural flows from USGS gauges was impossible. In a few instances, USGS gauges predated dams on tributaries of the Kennebec, so natural inflows were obtained for some historical period. For example, Flagstaff Lake was formed on the Dead River in 1948, while multiple USGS gauges existed on the Dead River as early as 1901. These early

records are useful in building a typical hydrograph for the reservoir inflows, but predate the energy price data which constitutes the other part of the SSDP trace.

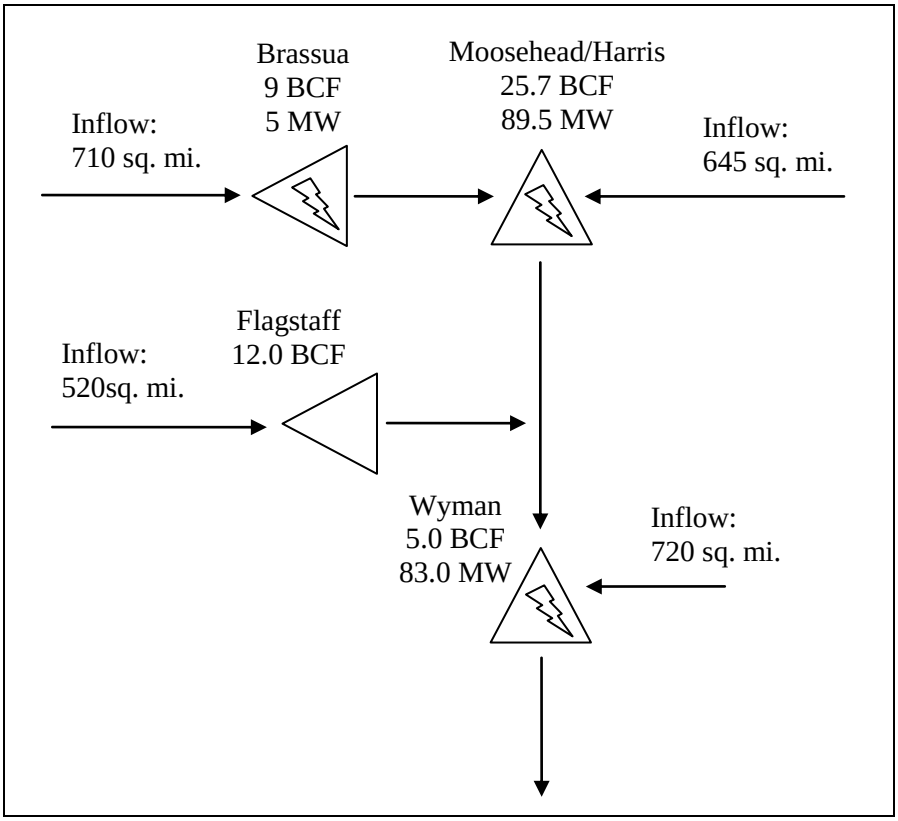

Figure 3: Schematic of Hypothetical System B

To obtain more recent natural inflow data, hourly flow records at USGS gauges on unobstructed local rivers were used as donor records. Slack et al. [1993] performed a survey of existing USGS streamflow records and identified sites which are free of regulation. Using this database, five candidate gauging stations were identified as having sufficiently long records, appropriate drainage areas, and proximity to upper Kennebec basins. These included the Sandy and Carrabassett rivers, which are tributaries to the Kennebec River, the Piscataquis and Mattawamkeag Rivers, which are tributaries to the adjacent Penobscot River, and the Allagash River.

It was important to ensure that the donor basins shared similar seasonal hydrologic characteristics with the reservoirs in the upper Kennebec basin. The primary annual hydrologic feature in rivers and streams in Maine is the spring freshet. In this study it was generally found that the spring freshet occurs later in the year the farther inland a basin lies. This is likely because coastal regions are generally more temperate than interior regions, and because many interior areas of Maine are mountainous. As part of the FERC licensing documentation, utilities must supply an average annual inflow hydrograph for each storage project. Thus, it was possible to compare the average natural inflow hydrograph for Brassua,

Moosehead, and Flagstaff Lakes to the average annual hydrographs for each of the candidate rivers. Overall, it was found that each of the candidate donor rivers generally matched the seasonal trend of the Upper Kennebec reservoir inflows. For example, Figure 4 plots the average annual hydrograph for Flagstaff Lake, along with the average annual hydrograph, scaled by drainage area, for USGS gauges on the Carrabassett and the Allagash Rivers.

It was observed that the timing and magnitude of the spring snowmelt runoff for the Allagash closely matched that for Flagstaff (when scaled), while the Carrabassett closely matches the summer-time flows. Thus, the Allagash was used as a donor site for the Spring and Winter months, while the Carrabasett was used for Summer months. Similar analyses were performed for each of the reservoirs on the Upper Kennebec.

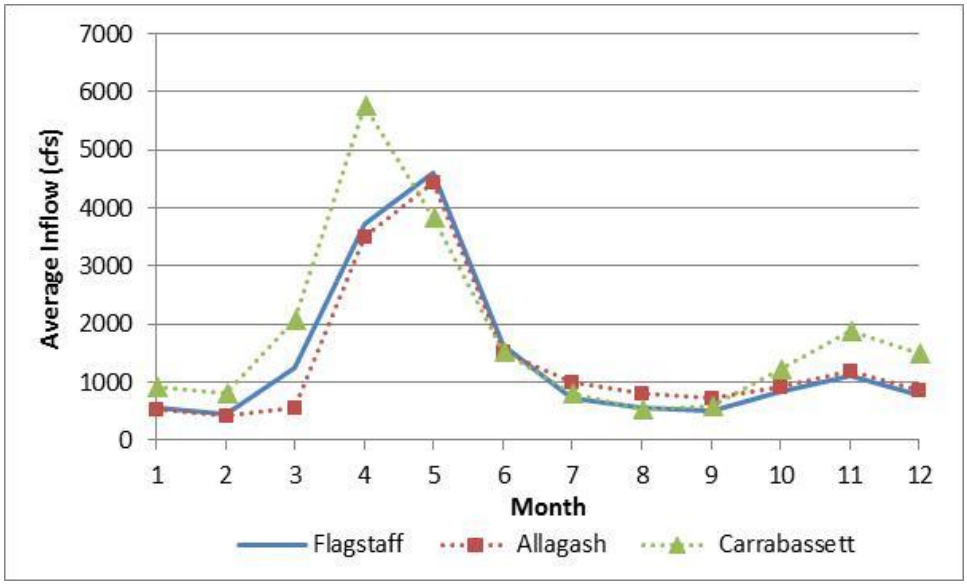

Figure 4: Average annual inflow hydrograph for Flagstaff Lake, with scaled average annual hydrographs for the Carrabassett and Allagash Rivers

It should be noted that by using hourly inflows from donor sites, we are losing the spatial correlation of the actual system. On the other hand, these are only meant to be hypothetical systems that approximate the Kennebec system, so this is deemed acceptable.

Section 3: Stochastic Dynamic Programming Algorithms Applied to Reservoir Operations

This section describes the application of dynamic programming algorithms to reservoir optimization. Recall from Section 1, that the objective in reservoir operations optimization is to maximize the benefit of operating the reservoir. In practice, time is often broken into discrete stages in which a release decision, R_t, must be made. Each R_t results in an incremental benefit B_t. The objective

is to select a sequence of R_t which maximizes the expected sum of the B_t plus the terminal value, v, from the present time $t = 1$ to the end of planning horizon $t = T$. This poses a difficult optimization problem because B_t is non-linear in R_t. Stochastic dynamic programming (SDP) is well suited to solving this problem because it determines an optimal sequence of decisions, can handle stochastic inputs, and has virtually no limitations on the functional form of the objective or the constraints.

In SDP applied to reservoir operations, the state of the system in each stage t is described by the storage, S_t. An additional variable, φ_t, which describes the hydrologic state of the system is often included [Loucks and Van Beek, 2005]. The hydrologic state variable might be the previous stage inflow [Little, 1955], a forecast for the next stage's inflow [Stedinger et al., 1984], or a combination of other relevant hydrologic measures [Cote et al., 2011]. A release R_t is selected for each state in each stage which maximizes the sum of B_t and the future benefit $f_{t+1}(S_{t+1})$. Note that $f_{t+1}(S_{t+1})$ is a function of the resulting state in the following stage, S_{t+1}. The SDP formulation which maximizes Z consists of the Functional Equation (2) and the Transitional Equation (3) [Faber and Stedinger, 2001]:

$$f_t(S_t, \varphi_t) = \max_{R_t} \left(B_t(S_t, R_t, Q_t) + \alpha \underset{\varphi_{t+1}|\varphi_t}{\mathrm{E}} [f_{t+1}(S_{t+1}, \varphi_{t+1}] \right) \quad \forall\, S_t \text{ and } t \in \{1, \ldots, T\} \tag{2}$$

$$S_{t+1} = S_t + Q_t - R_t - e_t(S_t, S_{t+1}) \tag{3}$$

where α is a discount factor and $e_t(S_t, S_{t+1})$ represents evaporation and seepage losses in stage t. The computation of equation (2) for the last decision stage T requires the terminal value of storage. Recall from equation (1) $f_{T+1}(S_{T+1}, \varphi_{T+1}) = v(S_{T+1}, \varphi_{T+1})$. An implicit assumption in the statement of equation (2) is that Q_t is known, allowing $B_t(S_t, R_t, Q_t)$ to be outside of the expectation. This simplifies the model formulation, and is a reasonable assumption in practice [Stedinger et al., 1984]. Another assumption in equation (2) is that the hydrologic state variable (often Q_t) is a Markov process. Because there is often a strong correlation between the hydrologic state variable in consecutive periods, conditioning the expectation in equation (2) on the current hydrologic state can better represent the hydrologic persistence of the system in time.

Equation (2) is solved with a backwards moving recursive procedure, i.e. (2) is solved successively for decision stages T, $T-1$, $T-2$,…, 2, 1. Numerical solution of SDP problems typically involves discretizing S_t, and the evaluation of equation (2) for each discrete S_t in each stage t [Loucks and van Beek, 2005].

An alternative to SDP is SSDP [Kelman et al., 1990]. SSDP differs from standard SDP in the representation of future inflows, and in the computation of f_t. While streamflow is represented in

equation (2) as a Markov process, SSDP represents future inflows as intact streamflow hydrographs, or traces. SSDP also separates the Functional equation into two parts: the Decision model (equation (4)) and the Evaluation model (equation (5)). Unlike standard SDP, which selects an optimal release and determines the value of that release with the same model, SSDP selects an optimal release with the Decision model, then determines the benefit from that release with the Evaluation model. The SSDP model which optimizes equation (1) is given by

$$\max_{R_t}\left\{B_t(S_t, Q_t(i), R_t + \alpha \underset{j|i}{E}[f_{t+1}(S_{t+1}, j)]\right\} \quad \forall\, S_t \text{ and } t \in \{1, \dots, T\} \tag{4}$$

$$f_t(S_t, i) = B_t(S_t, Q_t(i), R_t) + \alpha f_{t+1}(S_{t+1}, i) \quad \forall\, S_t \text{ and } t \in \{1, \dots, T\} \tag{5}$$

where $Q_t(i)$ is the reservoir inflow in stage t in trace i, and the expectation in equation (4) is conditioned on the probability of transitioning from trace i in time t to trace j in time $t+1$. The traces are indexed as $i = 1, \dots, m$. In this formulation, the hydrologic state variable is the current trace i. The transition probabilities used to compute the expectation in equation (4) are discussed in Section 4.2. Like SDP, SSDP is solved through a backwards recursion, starting at the end of the planning horizon (time index T) and moving backwards in time to the present time.

The backwards moving SSDP provides the analyst with the optimal release and the value of storage at discrete values for each decision stage. However the actual storage is unlikely to coincide with one of the discrete storage levels. One solution might be to interpolate between storage levels, but Tejada-Guibert et al. [1993] instead recommend a one-stage forward moving SDP re-optimization process. This step selects the optimal release given the current storage and reservoir inflow, and uses the backwards moving SSDP solutions as the terminal value of storage. This step is repeated at each decision stage. If one considers the current stage's flow to be known, and the latest flow forecast for the next stage is denoted H, the re-optimization step can be expressed

$$\max_{R_t}\left\{B_t(S_t, Q_t, R_t) + \alpha \underset{i|Q_t,H}{\mathrm{E}}[f_{t+1}(S_{t+1}, i)]\right\} \quad \forall t \in \{1, \dots, T\} \tag{6}$$

In this case, the expectation is conditioned on the probability of transitioning to scenario i given current reservoir inflow Q_t and the current flow forecast for the next stage inflow H.

Section 4: The Time Decomposition Algorithm

Time decomposition of the reservoir optimization problem into overlapping sub-problems with different time-steps and optimization horizons is well suited to the decision structure of real-time hydropower operations [Yeh, 1985]. The problem is essentially that we must optimize short-term (often hourly) operations in light of seasonal or even inter-annual objectives. With such a long planning horizon, modeling hourly operations is unnecessary, and often computationally infeasible. Furthermore, the long-term uncertainties and forecasts might be of little relevance to real-time operation. For example the forecasted price of crude oil in 5 years should influence the seasonal operation of a reservoir, but is likely of little concern on an hourly basis.

Karmouz et al. [2003] propose time decomposition as a solution to the multi-objective nature of many reservoirs. They propose four phases of optimization:

1. Long-term planning: annual horizon, monthly decision step
2. Mid-term planning: monthly horizon, weekly decision step
3. Short-term planning: weekly horizon, hourly decision step
4. Real-time operation: unit dispatching

They recommend using the monthly optimization model to derive an optimal release for each month, in light of long term objectives. The weekly model determines the optimal distribution of the allotted volume between each week of each month, and so on. Zahraie and Karmouz [2004] implement the proposed framework for a reservoir system in Iran, solving the long and medium term phases with SDP algorithms, and the short term phase with a DP algorithm.

A similar time decomposition algorithm has been applied to the Central Valley Project in California, which consists of 9 reservoirs, 9 power plants, 3 canals, and 4 pumping stations. This algorithm consists of a monthly model with a yearly planning horizon, a daily model with a monthly planning horizon, and an hourly model with a daily planning horizon [Yeh, 1979]. Similar hierarchical time decomposition models have been applied by the Tennessee Valley Authority [Shelton, 1979; Wunderlich, 1979] and by Hydro Quebec [Bechard et al., 1981].

Yeh et al. [1992] applied a time decomposition algorithm to the optimization of a hydrothermal power system in China. The algorithm consists of a monthly model, with a time horizon of one year; a daily model, with a time horizon of one month; and an hourly model, with a time horizon of one week. The models are updated with periodicity corresponding to the time step of the particular model. The shorter duration models represent the system in more detail than the longer duration models. The longer-duration models provide constraints for the shorter duration models.

Other examples of a time decomposition approach are given by Dudley and Burt [1973], Vedula and Mujumdar [1992], and Vedula and Kumar [1996] who consider inter- and intra-seasonal irrigation allocations from multi-use reservoirs.

Section 4.1: Proposed Contribution

In most previous time decomposition algorithms, the higher-level models have provided constraints for the lower-level models. For example, a monthly planning model will select an optimal volume of water to be released in each month, and the weekly planning model determines the optimal allocation of that volume across weeks. I propose a similar but somewhat unique approach. Rather than the higher-level models providing an optimal release for the lower-level models, it provides $v(S_{T+1})$ at the end of each lower-level planning horizon. This approach seeks to build on previous time decomposition algorithms while exploiting the clear advantages of SSDP in representing uncertainty when deriving an optimal strategy.

The proposed algorithm has three steps.

1. Long term: SSDP model with a weekly time step and a seasonal or annual horizon determines the value of storage in each week from the current time to the end of the planning horizon. This step is to be run once or twice per season, or as new information becomes available.
2. Medium term: SSDP model with a six-hour time step and a weekly horizon determines the value of storage in each six hour period in the coming week. This step is to be run each week, or as new information becomes available.
3. Short Term: A one step re-optimization is run at the start of each six-hour period to determine the optimal release for that period.

This algorithm has several advantages. First it allows for sub-daily optimization over a seasonal or annual planning horizon without incurring major computational effort. Second, by using SSDP rather than traditional SDP models, the algorithm uses a better representation of uncertainty, and a more realistic model of the persistence of flows (i.e. potential inflows are represented by realistic sequences rather than Markov processes). Also, the decomposition allows the analyst to use different forecast products which are available for different time scales. For example, a major concern in seasonal reservoir planning in Maine is the spring snowmelt, and snowmelt forecasts on a weekly or monthly basis are of great value to long-term planning. On the other hand, sub-daily variability is largely driven by rainfall runoff, so daily and hourly precipitation forecasts are of great value to short-term planning.

By varying the transition matrices used in each of the three algorithm steps, a wide variety of representations of uncertainty can be constructed. This allows examination of the utility of different uncertainty structures for hydropower optimization in variable hydrology.

Section 4.2: Transition Probabilities and Representation of Uncertainty

In SSDP the transition matrix describes the probability of transitioning from trace i in stage t to trace j in stage $t+1$. The choice of transition matrix dictates the representation of uncertainty in the optimization. If the transition matrix is the identity matrix, then transitions between traces are not considered and the optimization is deterministic. This will be referred to as the "I" case.

Alternatively, if every element of the transition matrix is $1/m$, where m is the number of traces, then it is equally likely that the system will transition into any trace in the next decision step. This will be referred to as the "M" case.

If the hydrologic state of the system is described by some variable, then it can be desirable to condition the transition probability between traces on that variable. Common hydrologic state variables are the current or previous decision stage inflow [Little, 1955; Loucks and van Beek, 2005]. Stedinger et al. [1984] use an inflow forecast as a hydrologic state variable for an SDP case study on the High Aswan Dam in Egypt. Kelman et al. [1990] and Faber and Stedinger [2001] use forecasts as hydrologic state variables for single reservoir SSDP applications in California and Colorado respectively. In this study, inflow forecasts for the next time period are used as hydrologic state variables. Thus, the probability of transitioning from trace i to trace j in time $t+1$ is conditioned on the inflow forecast in time t. This will be referred to as the "F" case.

Kelman et al. [1990] and Faber and Stedinger [2001] use a Bayesian method to estimate the transition probability between traces. The same procedure was adopted for this work. Each trace has unique inflow and forecast series, thus the probability of transitioning from trace i to trace j is equal to the probability of experiencing the flow from trace j given the forecast in trace i:

$$P_t[j|i] = P_t[Q_t(j)|F_t(i)] = P[j]\frac{P[F_t(i)|Q_t(j)]}{\sum_{k=1}^{m}(P[F_t(i)|Q_t(k)]P[k])} \quad (7)$$

A key feature is that the Bayesian likelihood function, $P[F_t(i)|Q_t(j)]$, takes into account both the forecasted volume and its precision. Thus more precise forecasts should result in a narrower likelihood function, and consequently an improved optimization. This point is explored later. Figure 5 shows an example of the transition probabilities assigned to 20 traces given the M and F transition matrix cases described above.

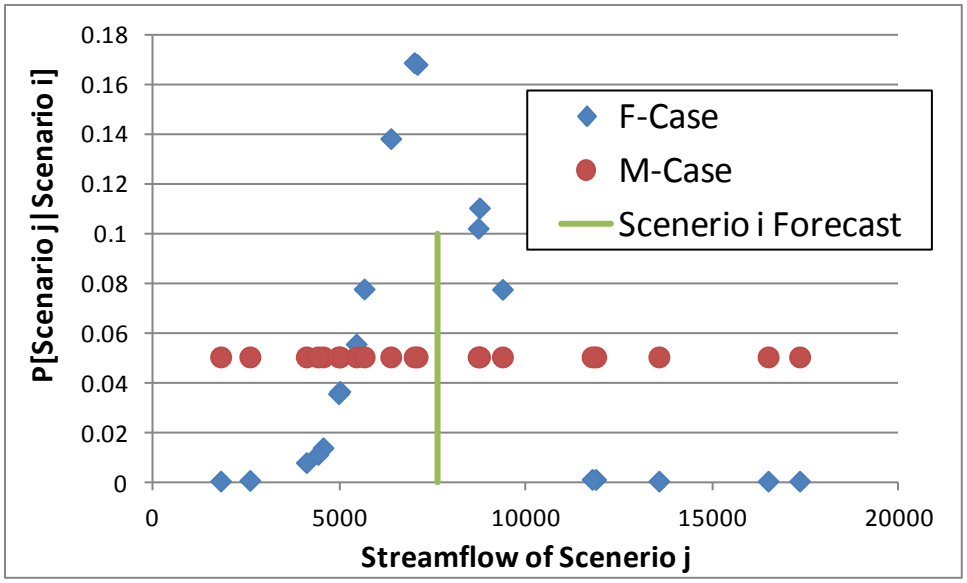

Figure 5: Probability of transitioning from scenario i to scenario j for the F and M cases vs. the streamflow volume in scenario j.

Given the three steps of the algorithm described in the previous section, it is possible to achieve a variety of representations of uncertainty by selecting the transition case for each step. For example, one might choose the "I" case for the both the backwards optimization steps, then the "M" case for the forwards re-optimization step. The resulting algorithm would referred to as the I/I/M configuration.

By comparing various model configurations we can draw general conclusions on the utility of different transition cases for the long-, mid-, and short-term planning in the variable hydrology of Northern New England. For example, we can examine whether using medium-term forecasts, say on a weekly scale, are of any value to the overall operation of the hydro system by comparing the performance of the I/M/F and I/F/F configurations. Initial findings suggest that forecasts are of the most value in the short-term re-optimization step, and are of little value for long- and medium-term planning.

Section 4.3: Initial Findings

The time decomposition algorithm proposed in Section 3.1 was applied to summer operations for the hypothetical System A described in Section 2.2.2. A variety of model configurations were applied. These configurations fall into three categories: configurations with no forecasts, configurations with forecasts for the re-optimization step only, and configurations with forecasts for all steps.

To measure the performance of each configuration, the 'perfect foresight' case was also considered. This corresponds to the I/I/I configuration. In this case, a deterministic backwards SSDP is used for the first two optimization steps, then re-optimization is performed with perfect foreknowledge of future flows. Table 1 reports the average summer benefit obtained from operating System A for each of

the configurations and the average efficiency over 20 years of simulated operation. Efficiency is the ratio of the summer benefit and perfect summer benefit.

Table 1: Summer Benefit and Efficiency for various configurations of the time decomposition algorithm applied to hypothetical System A

Configuration	Summer Benefit ($M)	Efficiency
M/M/M	8.23	0.965
I/I/M	8.25	0.968
M/M/F	8.27	0.969
I/I/F	8.33	0.977
F/F/F	8.34	0.978
Perfect	8.53	1

Remarkably, even configurations with no forecasts perform very well (M/M/M and I/I/M on the order of 97% efficient). This is because average summer flows in Maine are small compared to the available storage, so that variation in future inflows does not usually affect planning decisions. The I/I/M case returns a better result than the M/M/M case, likely because it better represents the persistence of flows in the backwards optimization steps.

As expected, using forecasts in the re-optimization step generally improves model performance. For example, the M/M/F case performs better than the M/M/M case. The I/I/F case performs significantly better than the M/M/F case. Again, this is likely because the I case has better persistence of flow, resulting in improved optimization results.

Adding forecasts to each optimization step improves the results. The fact that I/I/F performs nearly as well as F/F/F suggests that forecasts are of most benefit in the re-optimization, short term planning, at least for summer operations

Section 4.5: Discussion and Future Work in this area

The fact that the M/M/M and I/I/M cases perform so well is surprising. It is in part attributable to the hydrology of the Summer operations period considered. It is also a product of averaging benefits over the entire Summer season, and across 20 years of operation. During typical decision stages, each of configurations in Table 1 report nearly the same operating policy, but for the rare event that an extreme flow occurs, the configurations which used forecasts performed much better. These events occurred seldom enough during the simulation period to only slightly affect the average benefits. Thus even very simple and naïve configurations perform reasonably well on average, but may encounter problems during

extreme events. In fact, Faber and Stedinger [2001] report a similar result: configurations which used no forecasts performed at 92-94% efficiency when applied to full-year operations for a reservoir in Colorado.

It is interesting that the I/I/F configuration performs almost as well as the F/F/F configuration. It suggests that forecasts are of benefit for only the short-term re-optimization step. Furthermore, this also suggests that the shape of the decision tree after the current period is not important, so long as the future value function used to make the current period decision is reasonable. Faber and Stedinger [2001] also found that configurations which featured forecasts only in the re-optimization step performed as well as configurations which featured forecasts in each optimization step.

There are some areas where the current work could be expanded. The current time decomposition model does not accurately reflect the New England ISO's market structure. In the New England ISO there are both real-time and day-ahead energy markets, as well as ancillary service markets. In the day-ahead market, bids are placed the day before scheduled production. The real-time market is designed to accommodate changes from the day-ahead scheduled production [NE ISO, 2013]. The current time decomposition model ignores this market complexity and assumes one market value which is available at the time of production. It is also assumed that the market will except all energy produced by the system and that the system output will not influence the energy price. Given the small size of the Kennebec system, the second assumption seems reasonable, but future work will need to better reflect the two-tiered market structure.

Incorporating the two-tiered market will likely include the addition of a state variable representing the day-ahead commitment. The optimization will then decide whether to provide the scheduled energy or buy it on the real-time market.

A second point of research will be the generation of multivariate synthetic forecasts. The current work considers only an inflow forecast for a single reservoir. Future work will involve inflow forecasts for multiple reservoirs, and an energy price forecast. To generate these, the multivariate GMOVE proposed by Grygier et al. [1989] will be used. There has been significant work on energy forecasting in deregulated markets [Aggarwal et al., 2009], and this work must be reviewed before substantive progress on synthetic energy forecast can be made. Of course, the primary concern is ensuring the energy price forecasts have reasonable standard error of prediction, not in actual forecasting procedures per se.

Finally, full season model runs must be made. At present, all of the optimization runs have included only summer operations. This is because summer hydrology is generally more variable than

winter hydrology in Northern Maine. Full season runs should shed light on the relative merit of various decision tree structures in different seasons.

Section 5: Forecast Precision and Reservoir Optimization

This research does not use an existing forecast product, but instead uses synthetic forecasts created using the generalized maintenance of variance extension (GMOVE) proposed by Grygier et al. [1989]. This procedure was utilized to generate synthetic streamflow forecasts with the desired correlation to the actual streamflow. Assuming that the forecast is the product of a linear regression model, the R^2 is the square of the correlation of the forecasted flow and the actual flow. This allows us to consider the benefit of forecast precision to operations optimization. For example, how much do reservoir operations improve if forecasts with $R^2 = 0.95$ rather than $R^2 = 0.65$? We can examine this by comparing the I/I/F95 and I/I/F65 configurations, where F65 is the "F" case with $R^2 = 0.65$.

Another question is at what planning scale does forecast precision help the most. For example, is higher precision for sub-day planning more valuable than higher precision on a weekly scale. A related question is how the value of forecast precision at different time scales changes seasonally. In Maine, a major concern for long- and mid-term planning during the spring is the snowmelt runoff, whereas in the summer and fall a major concern is heavy rainfall from localized thunderstorms. Perhaps long-term forecast precision is more important during the spring and short-term precision in the summer. By taking advantage of the structure of the time decomposition algorithm these questions are explored.

Section 5.1: Initial Findings

Forecast with a variety of R^2 were generated and used in the time decomposition algorithm configurations reported in the previous part. These algorithms were then applied to the optimization of the summer operations of hypothetical System A. Table 2 reports the average summer benefit and the efficiency of model configurations with various uncertainty structures and varying forecast precision.

By comparing the M/M/F50 and M/M/F95 configurations, it is clear that using forecasts with higher precision yield improved optimization results. The I/I/F95 case performs significantly better than the M/M/F95 case. Again, this is likely because the I case has better persistence of flow, resulting in improved optimization results.

Adding forecasts to each optimization step generally improves the results. Interestingly, F50/F75/F95 performs as well as F95/F95/F95. This suggests that forecast precision is most important for the short-term re-optimization step, and is off little importance for longer term planning. The fact that

I/I/F95 performs nearly as well as F95/F95/F95 suggests that forecasts are of most benefit in the re-optimization, short-term planning, at least for summer operation.

Table 2: Summer Benefit and Efficiency for various configurations of the time decomposition algorithm applied to hypothetical System A, with varying forecast precision

Configuration	Summer Benefit ($M)	Efficiency
M/M/M	8.23	0.965
I/I/M	8.25	0.968
M/M/F50	8.24	0.966
M/M/F95	8.27	0.969
I/I/F95	8.33	0.977
F50/F50/F50	8.30	0.973
F50/F75/F95	8.34	0.978
F95/F95/F95	8.34	0.978
Perfect	8.53	1

Section 5.2: Discussion and Future Work in this area

So far, the work in this area has been limited, but it raises very interesting questions. Thus far, tests of the time decomposition algorithm have only included Summer operations. It was shown that forecasts and forecast precision are most important for the short-term, sub-daily optimization. This is not entirely surprising: the significant uncertainty in Summer operations is the arrival of localized, brief thunderstorms, so short-term forecasts are very important. However, during the Winter and Spring, a major uncertainty is the timing and quantity of the spring snowmelt runoff, which can act on a longer time scale. Thus, it is speculated that the value of long-term forecasts should be much greater in the Winter months than in the Summer months. Full year runs should reveal if this is true.

As stated earlier, future work will include multi-dimensional application of the time decomposition algorithm, which will require multi-dimensional forecast vectors. An interesting question to examine will be the effect of varying forecast precision across the system reservoirs. One could certainly imagine that forecast precision is not uniform across a wide basin, and that depending on the relative size of the reservoir storage and inflow improved precision may or may not be important. The system configuration will also likely play a large role in determining how varying forecast precision affects the overall optimization performance.

As described earlier, future work will also include energy price forecasts in the computation of transition probabilities. An interesting question is whether the precision of hydrologic or energy price forecasts is more important to the overall optimization effort. One suspects this will largely depend on the relative variability of the two, but how is not exactly clear.

Section 6: Corridor DP for high dimensional problems

SSDP holds great promise for multi-reservoir optimization problems. Because traces derived from historical flow records are used, the optimization will capture the spatial interrelationships among streamflows much better than traditional Markov streamflow models [Faber, 2000]. However, additional reservoirs typically requires the addition of state variables, thus incurring Bellman's "curse of dimensionality"[Bellman, 1961]. Suppose the SSDP problem includes k state variables (storage for k reservoirs), and each is discretized and evaluated at N points. Equation (4) must then be solved at N^k points in the k-dimmensional state space for each of the T decision stages. For example, Figure 6 shows a 3-dimensional representation of a 4-dimensional lattice with 10 discrete points in each dimension.

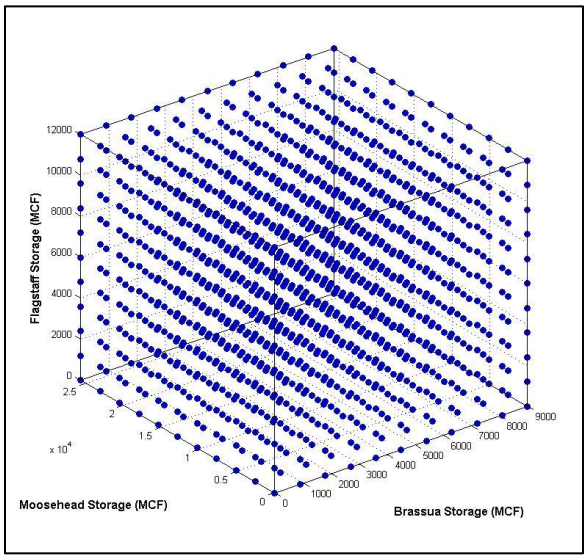

Figure 6: Lattice of Discrete points in a 4-dimensional continuous state space for a hypothetical hydro system, with 10-discrete points in each dimension.

One approach to combating this problem is aggregation/disaggregation, wherein multiple reservoirs are represented as a single reservoir [Gilbert and Shane, 1982; Turgeon and Charbonneau, 1995]. A potential downside of aggregation/disaggregation is that it can lead to inaccurate results because the optimized system is an approximation of the actual system.

Another approach to reduce the burden of high-dimensional SSDP is to use higher order interpolation surfaces for the future value function. Many SDP applications use simple linear interpolation to approximate the future value function between discrete points in the state space. Johnson et al. [1993] found that by using cubic splines, it was possible to achieve the same relative error as linear interpolation but with a many fewer points. This translated to significant reduction in computational burden for two reasons. First, N is allowed to be smaller, so equation (4) is solved fewer times. Second, cubic splines have continuous gradients, allowing for more rapid solution to equation (4). While use of

cubic splines can allow a coarser lattice, the computational burden of solving a multi-dimensional problem will still grow exponentially with dimension k.

It is easy to demonstrate that much of the volume of the state space represents storage vectors which are not reasonable. When a reservoir system is operated reasonably it is unlikely that one reservoir will be full while others are empty. This can be seen by simulating the hypothetical System B described in Section 2.2.2 using historical records of discharge from the actual Kennebec River. Each point in the left panel of Figure 7 is a vector of storages which the system visited when simulated. It is clear that the system tends to travel in a corridor and never visits much of the state space during the 20 years of simulation. Thus, a great deal of work can be avoided by developing the future value function across a set of reasonable storages, called a corridor.

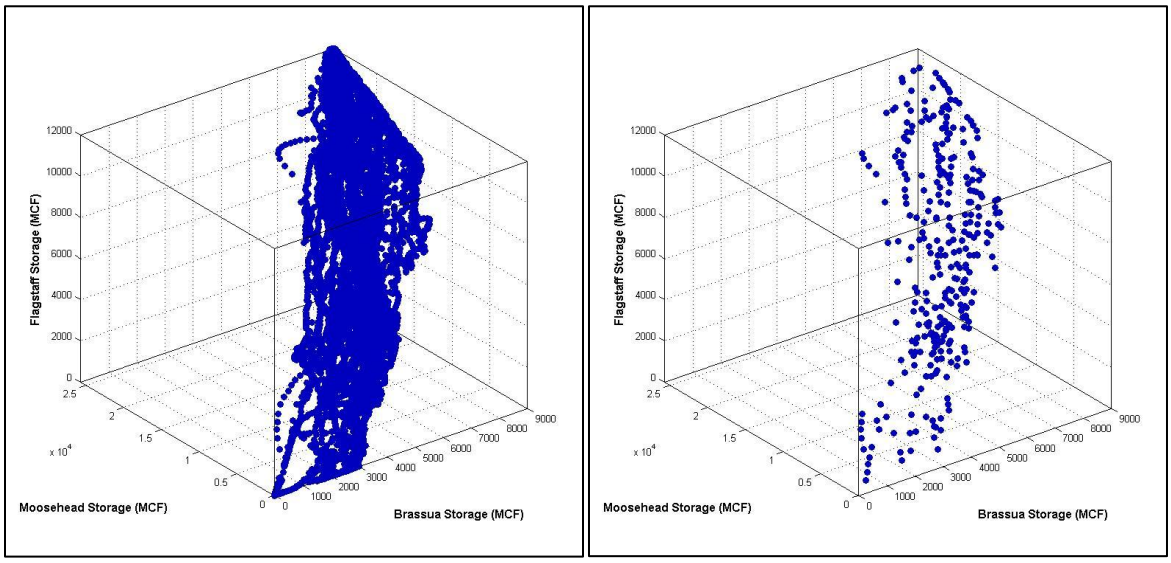

Figure 7: Path of a 4 reservoir system with the 4-dimensional state space over 20 years of simulation before trimming (left) and after trimming (right).

This concept has been explored by Pereira and Pinto [1985], who propose the Stochastic Dual Dynamic Programming (SDDP) algorithm. Their algorithm uses simulation of the system to obtain points where the future value function is evaluated. The future value function is approximated by piecewise linear Benders cuts. This involves iterative optimization and simulation till the desired precision is achieved. The linear approximation allows evaluation of the future value function over the entire volume of the state space. Remarkably, the Pereira and Pinto [1985] solve a 39 reservoir problem using this method. The SDDP model has also been successfully applied more recently [see Tilmant and Kelman, 2007; Goor et al., 2011]. We seek to extend the SDDP Corridor concept to SSDP. A major advantages of this is that SDDP requires a linear approximation of $f_t(S_t)$, while SSDP does not. Also SDDP is often paired with a Markov streamflow model, whereas SSDP uses intact streamflow traces.

Instead of evaluating the entire lattice of possible combinations of storage in the various reservoirs, a corridor will be developed containing those combinations of storage states that might reasonably be visited, or are near the solution for the operating decision developed for the current time. Pereira and Pinto [1985] developed their corridor by simulating the system iteratively as they derived their operating policy. Instead it is proposed to gather a compact set of reasonable system storage vectors from at least three sources:

(1) They may be storage vectors that occurred during the simulation of the historical streamflow record.
(2) They may be storage vectors obtained for the system over time as a result of simulating the system yesterday, or last week (which has the advantage that they should be very close to the values of interest when decisions are optimized today).
(3) They may be obtained by simulating the anticipated solution to the optimization model for today, perhaps with some perturbation of the initial storage volumes so as to generate a neighborhood of storage stages in the state-space near today's solution.

One reason that SDP applications have not taken advantage of the corridor idea is that the approximation techniques used to numerically solve the recursive equation, such as cubic splines or linear interpolation, work best on uniformly spaced k-dimensional lattices. New approximation techniques are potentially not as sensitive to the placement of discrete points in the state space. One such method is radial basis function (RBF) approximation [Regis and Shoemaker, 2007; Buhman, 2003]. The idea in Corridor DP with RBF approximation is to concentrate basis points within the corridor to achieve the desired precision in the important region of the state space with as few discrete points as possible. Initial trial runs of the Corridor DP algorithm are promising, and are discussed in Section 6.3. It is expected that better parameterization of the RBF surface will further improve overall performance. Good parameterization of the RBF surface is key to obtaining a good fit to the future value function. Efforts in this area are discussed in Section 6.2.

Section 6.1: Demonstration of the Corridor Concept

To demonstrate the corridor concept, streamflow records were used to simulate the operation of the hypothetical four reservoir System B from Section 2.2.2. The left panel in Figure 7 is a 3-dimensional representation of the path of the system over 20-years of simulated time in the 4-dimensional state space.

To obtain points which are more representative of the corridor than the simulated points one could 'thin' redundant points, then 'fill-in' the corridor. A point is redundant if it is very close to its nearest neighbor and essentially represents the same storage vector. It turns out that simple trimming approaches are inadequate, and more sophisticated approaches have been explored, as described in Section 6.2. Filling involves placing new points in the corridor region. Again, simple approaches to this gave poor results, so a more sophisticated approach has been taken. The right panel of Figure 7 is a 3-dimensional representation of the corridor for the 4-dimesnional simulated hypothetical system after

trimming. Observe that the extent of the corridor has largely been retained, but that many redundant (close) points have been eliminated. In practice, it is often necessary to iterate thinning and filling processes until an adequate and semi-uniform point density has been established through the corridor region. The left panel in Figure 8 is an example of a corridor after iterating between thinning and filling.

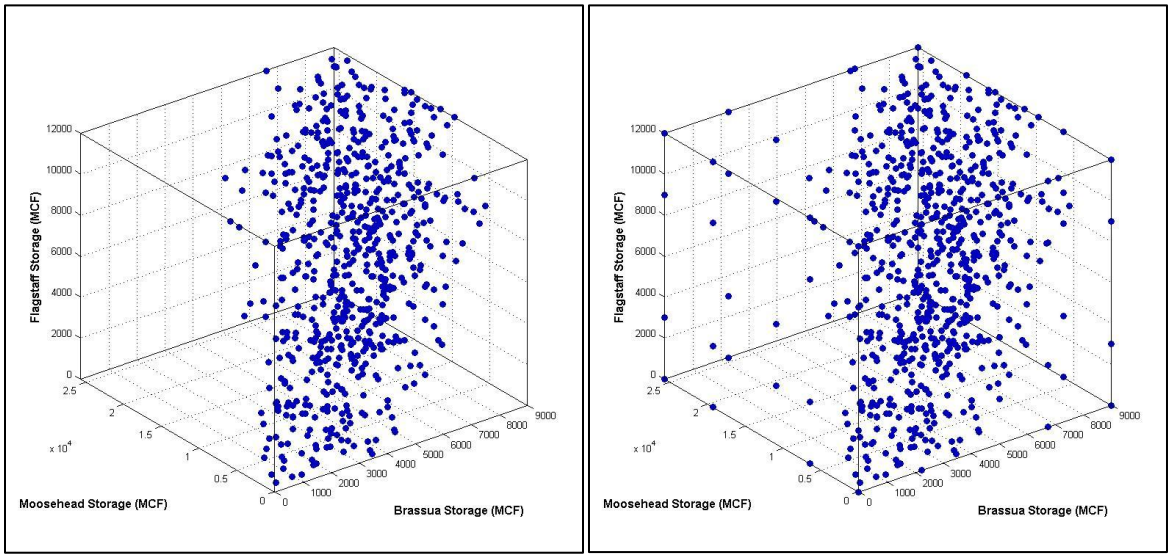

Figure 8: Corridor of a 4 reservoir system in the 4-dimensional state space after filling and re-trimming before adding the backbone (left) and after adding the backbone (right).

Though the optimization efforts are focused on the corridor, the SSDP algorithm is still searching the entire state space to solve equation (4). For this reason, it is important that the approximation of the future value function in the corners of the state-space is reasonably accurate. To accomplish this, it is advisable to add a coarse lattice in the extremes of the state space, a so-called 'backbone.' One recommendation for this is to simply add discrete points at 0, 25, 75, and 100% of full in each dimension of the state space. This will add 4^k points in the k-dimensional state space, but will help improve the overall performance of the optimization algorithm. The right panel of Figure 8 is a 3-dimensional representation of the 4-dimensional corridor with the 'backbone' added.

Section 6.2 RBF Tuning and Local Density inside the Corridor

One of the difficulties in using RBF surfaces to approximate the future value function is that small ripples in the surface can cause gradient-based search algorithms to terminate at non-optimal locations. Because SSDP is a recursive procedure, errors incurred by non-optimal solutions of equation (4) compound over time and end in very poor results.

These ripples can be eliminated by better parameterization of the RBF surface, and by more regular placement of the basis points in the corridor. Both are areas of ongoing research which are discussed briefly here.

RBF Parameterization

The radial basis function (RBF) approximation of function Y at point j in k-dimensional state-space is given by:

$$\hat{Y}_j = \sum_{i=1}^{N} \beta_i \phi\left(\left\|\boldsymbol{X}_i - \boldsymbol{X}_j\right\|\right) + p\left(\boldsymbol{X}_j\right)$$

where $\|\cdot\|$ is the Euclidean norm, $\beta_i \in \mathbb{R}$, N is the number of basis points, $\phi(\cdot)$ is the basis function, and $p(X)$ is some polynomial function of X. Basis functions can take several functional forms, as summarized in Table 3.

Table 3: Basis Functional Forms and Conditions

Name	Functional Form	Conditions
Surface Splines	$\phi(r) = r^{\kappa}$ $\phi(r) = r^{\kappa}\log(r)$,	$\kappa \in \mathbb{N}$, κ odd $\kappa \in \mathbb{N}$, κ even
Multiquadrics	$\phi(r) = (r^2 + \gamma^2)^{\kappa}$	$\kappa \notin \mathbb{N}$, $\kappa > 0$
Inverse Multiquadrics	$\phi(r) = (r^2 + \gamma^2)^{\kappa}$	$\kappa < 0$
Gaussian	$\phi(r) = e^{-\gamma r^2}$	$\gamma > 0$
Tri-cube	$\phi(r) = \max\left(0, \left(1 - \left(\frac{r}{B}\right)^3\right)^3\right)$	$B > 0$

Some functional forms, such as surface splines, have no parameter which controls the function scale. The Gaussian functional form has such a parameter, γ. As γ increases, the Gaussian function fades more quickly. The Tri-cube bandwidth parameter B has essentially the same purpose. At any distance greater than B, the function returns a value of zero.

Having such a parameter can be important in some cases. In our DP application, the density of points varies greatly across the state space. The RBF approximation is intended as a local approximation to model the deviations from a coarse spline surface fit to the backbone points. For this reason, it's unclear why every basis function should influence the approximation surface across the entire state-space. Furthermore, when surface spline RBFs were applied, near points began to look redundant and numerical problems were encountered when solving for $\boldsymbol{\beta}$. A good scale or bandwidth parameter can help address these concerns.

Since the density of points varies greatly across the state space, it is important to allow the bandwidth parameter to vary as well. Define point density at any arbitrary location i as

$$\rho_i = \frac{n}{CV} \tag{8}$$

Here CV is a k-dimensional control volume containing n basis points of M total basis points. For ρ_i to be meaningful, we must either fix CV or n across the state space. By fixing CV, we are defining the extent of the local density metric. In the extreme, the CV might encompass the entire state-space, in which case $\rho_i \propto M$, and ρ_i would become a global density rather than a local density. In the other extreme, a small CV might incorporate no basis points, which may or may not be desirable.

Alternatively, if n is fixed, and the CV is scaled to the required size to encompass n basis points, ρ_i becomes

$$\rho_i = \frac{n}{CV(n)} \tag{9}$$

Here $CV(n)$ is a k-dimmensional shape centered at point i and large enough to encompass exactly n points. Without specifying the shape of $CV(n)$, this definition is unsatisfactory: for a single n, ρ_i might take many values depending on how $CV(n)$ is defined. The following discussion will rely on two definitions of point density based on assuming a cubical or a spherical control volume.

Assuming a cubic control volume centered at point i the point density becomes:

$$\rho_{c,i} = \frac{n}{s^k} \tag{10}$$

where s is the cube side length. If n is fixed, $\rho_{c,i}$ becomes:

$$\rho_{c,i} = \frac{n}{s(n)^k} \tag{11}$$

where $s(n)$ is the side length of a cube centered on point i which encompasses exactly n basis points. If CV is a k-sphere centered at point i, then the point density becomes

$$\rho_{s,i} = \frac{n}{V_k(R)} = \frac{n}{a(k)R^k} \tag{12}$$

The volume of a k-sphere with radius R, $V_k(R)$, is the k^{th} power of R multiplied by a constant $a(k)$. For $k = 1, \cdots, 4$, Table 4 reports formulas for $V_k(R)$ and $a(k)$.

If n is fixed, $\rho_{s,i}$ becomes

$$\rho_{s,i} = \frac{n}{V_k\left(R_{(n)}\right)} = \frac{n}{a(k)R_{(n)}^k} \tag{13}$$

where $V_k\left(R_{(n)}\right)$ is the volume of a k-sphere with radius $R_{(n)}$, or the Euclidean distance to the n^{th} nearest basis point. This is an attractive definition because the RBF bandwidth parameter will assign non-zero function values within a spherical volume. Having defined local density at an arbitrary point i, how should the basis function bandwidth change with density, for a fixed dimension k?

Table 4: Volume of $\boldsymbol{k}$-spheres for various k

k	$a(k)$	$V_k(R)$
1	2	$2R$
2	2π	$2\pi R^2$
3	$\frac{4}{3}\pi$	$\frac{4}{3}\pi R^3$
4	$\frac{1}{2}\pi^2$	$\frac{1}{2}\pi^2 R^4$

First imagine a k-dimensional cubic control volume, CV, containing n basis points where each basis point is located at a cube vertex. Let $n = m^k$, so that each basis point is on the vertex of an $m \times m \times \cdots \times m$ lattice. The average Euclidean distance between basis points is then given by:

$$\sqrt{k\left(\frac{s}{m}\right)^2} = \sqrt{k}\frac{s}{m} = \sqrt{k}\frac{s^{k\frac{1}{k}}}{n^{\frac{1}{k}}} = \sqrt{k}{\rho_{c,i}}^{-\frac{1}{k}} \tag{14}$$

For a fixed k, the average Euclidean distance between basis points is proportional to $\rho^{-\frac{1}{k}}$. This implies that if bandwidth is to reflect the Euclidean distance between points it should be proportional to $1/\rho^{\frac{1}{k}}$. This should not depend on the shape of the control volume. Define,

$$B_i = \frac{b_1}{{\rho_i}^{\frac{1}{k}}} \tag{15}$$

for some constant b_1. B_i is the bandwidth parameter of the basis function centered at point i. In radial basis function applications, the control volume is typically a k-sphere. For spherical control volumes $B_i$becomes,

$$B_i = \frac{b_1}{{\rho_{s,i}}^{\frac{1}{k}}} = b_1\left[\frac{n}{a(k)R^k}\right]^{-\frac{1}{k}} = b_1\left[\frac{a(k)}{n}\right]^{-\frac{1}{k}}R \tag{16}$$

For a fixed k and n, $B_i \propto R_{(n)}$. This is a powerful result because it provides guidance about how one might vary the B_i parameter across the state space if the density of points varies. However, There are two parameters which must be specified: b_1 and n. There is some theoretical basis for the selection of n. Note that $R_{(n)}$ is an order statistic of R. In normal distributed samples, the variance of the order statistics decreases as you approach the median. Clearly R is not normal distributed, but the dimensionless variation (σ^2/μ^2) should decrease as one approaches the median. This implies that if a typical M is

between 300 and 400 points, a reasonable n might be between 50 and 100. If n is too large $\rho_{s,i}$ ceases to be a local density.

There is no clear theoretical value of b_1, except that $b_1 > 0$. This would dictate that as $R_{(n)}$ increases b_1 should also increase, or equivalently as $\rho_{s,i}$ decreases, B_i increases. Numerical optimization is used to determine a reasonable value of b_1.

The strategy proposed is to create several synthetic future value function surfaces of increasing complexity. A variety of RBF functional forms, and combinations of b_1, n, and N will be fit to each surface. Because the surface is synthetic, the true future value of water, and its first and second derivative are known at each point in the state-space. This allows a more thorough evaluation of the merits of each RBF parametrization. Also, since the surface is not known with certainty in reality, using approximate numerical solutions, from perhaps a high resolution spline solution, can introduce undesired numerical errors into the analysis.

The approximate surface is generated using the transformation developed for diagnostic purposes, which transforms every point in the 4-D state-space into 1-D. The transformation is:

$$T_i = \boldsymbol{a}\boldsymbol{C}_i = [0.3625 \quad 0.3279 \quad 0.1550 \quad 0.1545]\begin{bmatrix} C_i(1) \\ C_i(2) \\ C_i(3) \\ C_i(4) \end{bmatrix} \tag{17}$$

where $\boldsymbol{a}$ is a vector of weights, and $\boldsymbol{C}_i$ is a vector of storages in each of the four reservoirs in the hypothetical System B. Experience shows that when the future value function is projected in the transformed space, it is well approximated by a monotonic polynomial. By varying the order of the polynomial, and its coefficients, realistic synthetic surfaces of varying levels of complexity can be generated.

Local Density and Thinning and Filling

The concept of local density is also useful for thinning and filling the corridor. The initial thinning technique involved a simple distance threshold. In point pairs whose distance was less than the threshold, one point was dropped. Filling then involved generating new points by adding multivariate normal deviations to each retained point vector. This thinning and filling technique was iterated till an adequate coverage in the corridor was achieved. This approach resulted in clusters and holes in the corridor coverage which led to poor optimization results.

An alternative approach is to thin and fill points to achieve a semi-uniform point density through the corridor region. This could be implemented in several ways. First, a control volume of pre-specified

size might be placed about each corridor point. Points would then either be randomly added within the control volume or thinned, depending on if the density was smaller or greater than the desired density. The process would iterate until all points had the desired point density. Alternatively, n might be fixed and the control volume varied to encompass n points. If the control volume is larger or smaller than desired, points would be added or removed from the control volume. This process would also be iterated until the desired point density is achieved for every corridor point.

The first approach has been taken, though either approach should work. Initial trials indicate the density based approach for thinning and filling results in better optimization results than the threshold based approach.

Section 6.3 Initial Results

While there is still much work to do improving the implementation of the Corridor DP algorithm, initial trial runs are very promising. Trial runs have been conducted on the hypothetical System B from Section 2.2.2. This involves optimizing the 4-D system using three deterministic DP algorithms: standard DP with linear interpolation (hereafter referred to as Linear DP), standard DP with spline interpolation (Spline DP), and Corridor DP with RBF interpolation and a backbone spline (Corridor DP).

This simple test case involved three recursive steps backwards, i.e. $T = 3$. Each of the DP algorithms was solved using a range discretization levels, from 16 sampled points in the state space to 6561 points. The future value function in $t = 1$ from the highest density Spline DP was designated the true surface: f_{true}. The objective is to achieve a good approximation of f_{true} inside the corridor region. This is assessed by considering each approximation of the future value function at a set of P test points inside the corridor region, which are unique from the points used by any of the Corridor DP algorithms. The objective is then to match the value of f_{true} at each of the P test points. A measure of how closely a DP algorithm is matching f_{true} is to compute the scaled mean square relative error (scaled MSRE). Let $f_{j,M}$ be the future value function in time $t = 1$ of the j algorithm (j = Linear DP, Spline DP, or Corridor DP), and where M is the number of discrete points in state space which are sampled in the optimization. The scaled MSRE is then computed as:

$$Scaled\ MSRE = \frac{1000}{P}\sum_{p=1}^{P}\left(\frac{f_{true}(X_p) - f_{j,M}(X_p)}{f_{true}(X_p)}\right)^2 \tag{18}$$

Here X_p is the four-dimensional coordinate vector of the p^{th} test point. The scaling is necessary because the MSRE were very small in this simple test case, and were difficult to compare. The hope is that the Corridor DP can achieve a comparable scaled MSRE to Spline DP with a much smaller M. This would mean that for the same computational effort (approximately proportional to M), the Corridor DP achieves

a more accurate approximation of the future value function. Conversely, this means that the Corridor DP algorithm can achieve the desired accuracy with less effort. Table 5 lists the scaled MSRE for various M for the three DP algorithms considered.

Table 5: Scaled MSRE for three DP algorithms solved with different discretization levels

Basis Points	Linear DP	Spline DP	Corridor DP*
16	180.337	180.321	-
81	34.292	14.668	2.954
256	10.963	1.404	0.691
625	4.912	0.337	0.224
1296	2.131	0.174	0.089
2401	0.699	0.126	-
4096	0.485	0.053	-
6561	0.406	0.000	-

* Approximate MSRE

The Corridor DP scaled MSREs are approximate because the discretization levels for the Corridor DP did not coincide exactly with those for the Linear and Spline DP. As was hoped, the Corridor DP achieves a smaller scaled MSRE than Spline DP for the same discretization level. This means, for example, that with 1296 basis points, the Corridor DP achieves a scaled MSRE significantly smaller than that for Spline DP with 2401 points. This translates to an approximate speed up of over 2: it takes ½ the computational effort of Corridor DP to achieve the same relative error as Spline DP.

Section 6.4 Discussion and Future Work

At present, the Corridor DP is able to achieve the same relative error as Spline DP with about half of the computation time. This is exciting as a proof-of-concept example, but it is expected that through increased attention to corridor selection and RBF parameterization, Corridor DP can do even better. Another area of improvement on Corridor DP is for the algorithm to return the analytical gradient at each corridor point. This is one of the great strengths of SDDP: not only does it obtain the value of the future value function, it also returns the gradient. This should decrease the time needed to solve equation (4) at each iteration, and should also reduce the number of discrete points needed. Finally, the current SSDP model contains many complex constraints. While realistic, these constraints are causing numerical problems in solving equation (4). Many diagnostic tools have been developed to identify when errors occur, but this is ultimately a patch and not a solution to the problem. As this is intended to be a 'proof of concept' trial, an alternative SSDP model where many of the constraints have been relaxed should be implemented. This should help Corridor DP perform well, and will showcase the merits of the algorithm.

Section 7: Conclusions

This report is a summary of the research which has been conducted while supported by the HRF fellowship. The general topic is reservoir operations optimization, primarily using DP algorithms. Within this topic are three areas of concern. The first is on a time decomposition algorithm intended for near real time hydropower optimization. This algorithm relies on three nested optimization models, wherein the higher level models provide the future value of water to the lower level models. Using this model, the relative merit of different representations of uncertainty are explored. Ultimately it was shown that configurations which use forecasts for short-term decision making are most successful. Additionally, it is important that the longer-term models use an adequate representation of the persistence of flow in the basin. The second research concern is the value of forecast precision to the overall optimization effort. The examination of this involves the generation of synthetic flow forecasts of varying precisions. It is shown that forecast precision in the short-term are most important to overall reservoir optimization. The third research concern is the reduction of the computational burden of high-dimensional SSDP problems. This is achieved by focusing the optimization effort on the corridor in the state space where the reservoir system is most likely to travel. Initial findings show that computational savings are possible, and it is hoped through better parameterization of the RBF surface that further improvements can be made.

Works Cited

Aggarwal, S.K., Lalit, M.S., Kumar, A., Electricity price forecasting in deregulated markets: A review and evaluation, Electrical Power and Energy Systems, 31, 13-22, 2009.

Becker, L., and W. W-G. Yeh, Optimization of Real Time Operation of a Multiple-Reservoir System, *Water Resour Res*, 10(6), 1107-1112, 1974.

Bechard, D., et al., The Ottawa River regulation modeling system (ORRMS), in *Proceedings of International Symposium on Real-Time Operation of Hydrosytems*, vol. 1, pp. 1979-198, University of Waterloo, Waterloo, Ont., 1981.

Bellman, R.E.(1961). *Adaptive Control Processes*. Princeton University Press, Princeton, NJ.

Buhmann, M.D. (2003). *Radial Basis Functions*. Cambridge University Press, New York, N.Y.

Côté, P., D. Haguma, R. Leconte, S. Krauc, Stochastic optimization of Hydro- Quebec hydropower installations: a statistical comparison between SDP and SSDP methods, *Canadian Journal of Civil Engineering*, 38:(12) 1427-1434, 10.1139/l11-101, 2011.

Dudley, N. J., O. R. Burt. (1973). "Stochastic Reservoir Management and System Design for Irrigation." *Water Resour Res*., 9(3), 507-522.

Faber, B.A., Reservoir Optimization Using Sampling Stochastic Dynamic Programming (SSDP) with Ensemble Streamflow Prediction (ESP) Forecasts, PhD thesis, Cornell University, Sept. 2000.

Faber, B.A., and J.R. Stedinger, Reservoir optimization using sampling SDP with ensemble streamflow prediction (ESP) forecasts, *J. of Hydrology 249*(1-4), 113- 133, 2001.

Gilbert, K.C, and R.M. Shane, TVA hydro scheduling model: Theoretical aspects, *J. of Water Resource Planning and Management, 108* (WRI), pp 21-36, 1982.

Goor, Q., Kelman, R., and Tilmant, A., Multipurpose-Multireservoir Operation Model with Variable Productivity of Hydropower Plant, *J. Water Resour. Plann. Manage.*, 137(3), 258–267. doi: 0.1061/(ASCE)WR.1943-5452.0000117, 2011.

Grygier, J.C., Stedinger, J.R., Yin, H-B, A Generalized Maintenance of Variance Extension Procedure for Extending Correlated Series, *Water Resour. Research*, 25(3),345-349,1989.

Hodgkins, G.A., James II, I.C., Huntington, T.G., Historical Changes in Lake Ice-Out Dates as Indicators of Climate Change in New England, 1850-2000. *Int. J. Climatol*. 22: 1819-1827, 2002.

Hodgkins, G.A., Dudley, R.W., Loiselle, M.C., 2005, Historical Late-Winter and Spring Snowpack Depth and Equivalent Water-Content Data for Maine: U.S. Geological Survey Open-File Report 2005-1259, 80 p.

Johnson, S.A., J.R. Stedinger, C.A. Shoemaker, Y. Li, J.A. Tejada-Guibert, Numerical Solution of Continuous-State Dynamic Programs Using Linear and Spline Interpolation, *Operations Research*, Vol. 41, No. 3, May-June 1993.

Karamouz, M., F. Szidarovszky, B. Zahraie. (2003). *Water Resources Systems Analysis*, Lewis Publishers, New York, N.Y.

Kelman, J., J. R. Stedinger, L. A. Cooper, E. Hsu, S-Q. Yuan. (1990). "Sampling stochastic dynamic programming applied to reservoir operation." *Water Resour. Res.*, 26(3), 447-454.

Kennebec Water Power Co. *Maine's Mutliple-Use River: Kennebec River—Past and Present*. Kennebec Water Power Co.

Labadie, J. W., Optimal Operation of Multi-Reservoir Systems: State-of-the-Art Review. *J. of Water Resources Planning and Management* , 130(2), 93-111, (doi: http://dx.doi.org/10.1061/(ASCE)0733-9496(2004)130:2(93)), 2004.

Little, J.D.C., "Use of Storage Water in a hydroelectric System", J. *of Operations Research*, 3, 187-197, 1955.

Loucks, D., and van Beek, E. (2005). *Water resources systems planning and management: An introduction to methods, models and applications*, J. Stedinger, J. Dijkman, and M. Villars, eds., UNESCO Publishing/WL-Delft Hydraulics, Paris.

National Atlas of the United States, 2005.

New England ISO, 2013, How Our Markets Work, accessed 15 October 2013, <http://www.iso-ne.com/nwsiss/grid_mkts/how_mkts_wrk/index.html>.

Pereira, M. V. F., and Pinto, L. M. V. G., "Stochastic optimization of a multireservoir hydroelectric system: A decomposition approach." *Water Resour. Res., 21(6)*, 779–792, 1985.

Regis, R.G., Shoemaker, C.A., A Stochastic Radial Basis Function Method for the Global Optimization of Expensive Functions, *Informs Journal on Computing*, 19(4), pp. 497-509, 2007.

Shelton, R.A., Management of TVA reservoir systems, paper presented at Proceedings of the National Workshop on Reservoir Systems Operations, Univ. of Colo., Boulder, Aug. 13-17, 1979.

Slack, J.R., Lumb, A.M., Landwehr, J.M., 1993. Hydro-climatic data network: streamflow data set. U.S. Geological Survey Water Resources Investigation Report 93-4076. U.S. Geological Survey, Reston, Virginia.

Stedinger, J. R., Sule, B.F., Loucks, D.P. (1984). "Stochastic dynamic programming models for reservoir operation optimization." *Water Resour. Res.*, 20(11), 1499-1505.

Tejada-Guibert, J. A., S. A. Johnson, J. R. Stedinger. (1993). "Camparison of two approaches for implementing multireservoir operating policies derived using stochastic dynamic programming." *Water Resour. Res.*, 29(12), 3969-3980.

Tilmant, A., and Kelman, R., "A stochastic approach for analyzing trade-offs and risks associated with large-scale water resources systems." *Water Resour. Res., 43,* W06425, 2007.

Turgeon, A. and R. Charbonneau, An aggregation-disaggregation approach to longterm reservoir management, *Water Resour. Res.*, 34(12), 3585-94, 1995.

Vedula, S., and P. P. Mujumdar (1992). "Optimal reservoir operation for irrigation of multiple crops." *Water Resour. Res*. 28(1), 1-9.

Vedula S. and D. N. Kumar (1996). "An integrated model for optimal reservoir operation for irrigation of multiple crops." *Water Resour. Res.*, 32(4), 1101-1108.

Wunderlich, W.O., Planned enhancement of water management methods for the TVA reservoir system, paper presented at Proceedings of the National Workshop on Reservoir Systems Operations, Univ. of Colo., Boulder, Aug. 13-17, 1979.

Yeh, W.W-G., Real-time reservoir operation: The California Central Valley Project case study, paper presented at Proceedings of the National Workshop on Reservoir Systems Operation, Univ. of Colorado, Boulder, Aug. 13-17, 1979.

Yeh, W. W-G. (1992). "Optimization of real-time hydrothermal system operation." *J. Water Resour. Planning and Mgmt*., 118(6), 636-653.

Yeh, W.W-G.(1985)." Reservoir Management and Operations Models: A State-of-the-Art Review." *Water Resour. Res.*, 21(12),1797-1818.

Zahraie, B. and M. Karamouz (2004). "Hydropower reservoirs operation: A time decomposition approach." *Scientia Iranica*, 11(1-2), 92-103.